Water Research 247 (2023) 120808

Contents lists available at ScienceDirect

Water Research

journal homepage: www.elsevier.com/locate/watres

N-containing dissolved organic matter promotes dissolved inorganic carbon supersaturation in the Yangtze River, China

Lize Meng [a,b,c,d,$], Jingya Xue [a,b,c,d,$], Chu Zhao [a,b,c,d], Tao Huang [a,b,c,d,*], Hao Yang [a,b,c,d], Kan Zhao [a,d], Zhaoyuan Yu [a,b,c,d], Linwang Yuan [a,b,c,d], Qichao Zhou [h], Anne M. Kellerman [e], Amy M. McKenna [f,g], Robert G.M. Spencer [e], Changchun Huang [a,b,c,d,*]

[a] Jiangsu Center for Collaborative Innovation in Geographical Information Resource Development and Application, Nanjing Normal University, Nanjing 210023, PR China
[b] State Key Laboratory Cultivation Base of Geographical Environment Evolution (Jiangsu Province), Nanjing 210023, PR China
[c] Key Laboratory of Virtual Geographic Environment (Nanjing Normal University), Ministry of Education, Nanjing 210023, PR China
[d] School of Geography, Nanjing Normal University, Nanjing 210023, PR China
[e] Department of Earth, Ocean and Atmospheric Science, Florida State University, Tallahassee, FL 32306, USA
[f] National High Magnetic Field Laboratory, Florida State University, Tallahassee, FL 32310, USA
[g] Department of Soil and Crop Sciences, Colorado State University, Fort Collins, CO 80523, USA
[h] Institute for Ecological Research and Pollution Control of Plateau Lakes, School of Ecology and Environmental Sciences, Yunnan University, Kunming 650500, PR China

ARTICLE INFO

Keywords:
Dissolved organic matter
Organic sourced dissolved inorganic carbon
FT-ICR MS
Stable carbon isotopes

ABSTRACT

Dissolved inorganic carbon (DIC) represents a major global carbon pool and the flux from rivers to oceans has been observed to be increasing. The effect of weathering with respect to increasing DIC has been widely studied in recent decades; however, the influence of dissolved organic matter (DOM) on increasing DIC in large rivers remains unclear. This study employed stable carbon isotopes and Fourier transform ion cyclotron mass spectrometry (FT-ICR MS) to investigate the effect of the molecular composition of DOM on the DIC in the Yangtze River. The results showed that organic matter is an important source of DIC in the Yangtze River, accounting for 40.0 ± 12.1 % and 32.0 ± 7.2 % of DIC in wet and dry seasons, respectively, and increased along the river by approximately three times. Nitrogen (N)-containing DOM, an important composition in DOM with a percentage of ~40 %, showed superior oxidation state than non N-containing DOM, suggesting that the presence of N could improve the degradable potential of DOM. Positive relationship between organic sourced DIC (DIC_{OC}) and N-containing DOM formulae indicated that N-containing DOM is crucial to facilitate the mineralization of DOM to DIC_{OC}. N-containg molecular formular with low H/C and O/C ratio were positively correlated with DIC_{OC} further verified these energy-rich and biolabile compounds are preferentially decomposed by bacteria to produce DIC. N-containing components significantly accelerated the degradation of DOM to DIC_{OC}, which is important for understanding the CO_2 emission and carbon cycling in large rivers.

1. Introduction

Rivers play a substantial role in the global carbon cycle by not only exporting carbon but also outgassing carbon (C) from terrestrial systems enroute to the ocean (Cole et al., 2007; van Hoek et al., 2021). Previous studies have estimated that approximately 0.7–1.3 Pg C yr^{-1} of terrestrial C is delivered to the ocean (Drake et al., 2018), and 0.8–3.3 Pg C yr^{-1} of CO_2 is emitted from rivers to the atmosphere (Cole et al., 2007; Drake et al., 2018; Aufdenkampe et al., 2011; Raymond et al., 2013). As the dominant component of fluvial C and the dominator of riverine CO_2 emissions, dissolved inorganic carbon (DIC) contributes ~41 % of the total global C flux from rivers to oceans (van Hoek et al., 2021; Huang et al., 2012) and controls the supersaturated state of the partial pressure of carbon dioxide (pCO_2) in most rivers (Raymond et al., 2013). DIC is an indispensable participant in aquatic photosynthesis, pH regulation, and elemental cycles such as calcium, silicon, and magnesium (Köhler et al.,

* Corresponding authors: Changchun Huang and Tao Huang, Department of Geography, Nanjing Normal University, Wenyuan Road 1#, Qixia District, Nanjing, Jiangsu Province, PR China.
E-mail addresses: taohuang@njnu.edu.cn (T. Huang), huangchangchun@njnu.edu.cn (C. Huang).
$ Authors with equal contribution

https://doi.org/10.1016/j.watres.2023.120808
Received 28 June 2023; Received in revised form 24 October 2023; Accepted 28 October 2023
Available online 28 October 2023

2010; Tank et al., 2018; Kaushal et al., 2013). Alterations in DIC concentration and export will significantly affect aquatic physicochemical properties and carbon balance in riverine and land-ocean systems (Martin 2017; Raymond and Hamilton 2018; Song et al., 2021). Consequently, variability in concentration, sources, and corresponding drivers of riverine DIC has been increasingly recognized as an important component of biogeochemical processes in riverine and global carbon cycling.

Over recent decades, a substantial increase in DIC export from land to ocean, and the maintenance of the supersaturated state of pCO_2 in rivers has been proposed (Raymond and Hamilton 2018; Ren et al., 2015). Previous studies have reported that ~0.35 Pg C yr^{-1} DIC is delivered to the ocean (Huang et al., 2012; Cai 2011) and anthropogenically enhanced DIC flux of the Mississippi River in the past 50 years (Raymond et al., 2008). Mineral weathering (silicate and carbonate rocks), atmospheric dissolution, and organic matter degradation are the primary sources of DIC in rivers, with the hydrogen carbonate ion (HCO_3^-) being dominant in most natural waters (Tank et al., 2018; Chen et al., 2021a). The contributions of weathering, organic matter (OM), and atmospheric dissolution of CO_2 to DIC can be distinguished by the ^{13}C isotope of DIC ($\delta^{13}C_{DIC}$) due to the significantly more depleted and enriched $\delta^{13}C$ of dissolved OM (DOM) and carbonate (Ishikawa et al., 2015; Herath et al., 2022). The soluble products of DIC from enhanced chemical weathering generate more riverine DIC, which is regarded as the primary contributor to increased DIC (Köhler et al., 2010; Moosdorf et al., 2014; Taylor et al., 2016). The CO_2 from OM decomposition significantly contributes to the DIC in less weathered zones by dissolving and participating in carbonate equilibrium (Richey et al., 2002; Mayorga et al., 2005). The metabolism of river ecosystems shifts a large amount of organic to inorganic carbon, becoming the significant contributor to the carbon dioxide emissions (Battin et al., 2023). According to an incomplete estimation, the mean annual metabolic fluxes (include autotrophic and heterotrophic respiration) are 760 g C m^{-2} yr^{-1}, 591 g C m^{-2} yr^{-1} and 827 g C m^{-2} yr^{-1} for tropical, temperate, and high-latitudinal rivers, respectively (Battin et al., 2008; Appling et al., 2018; Gounand et al., 2018; Marzolf and Ardón 2021; Bernhardta et al., 2022). Light, flow, land use and climate change have been identified as primary drivers of river metabolism and carbon biogeochemistry (Bernhardta et al., 2022). Increased anthropogenic influences, such as mining exploitation, agricultural cultivation, urbanization, and industrialization, further intensify DIC input (Köhler et al., 2010; Raymond and Hamilton 2018), as well as alter the organic matter (OM) molecular composition and thus its environmental role and fate (Williams et al., 2016; Vaughn et al., 2021; Zhou et al., 2022). The influence of rock chemical weathering on riverine-increased DIC deserves attention for its role as a carbon sink (Tank et al., 2018; Raymond and Hamilton 2018; Ren et al., 2015). However, the effect of the molecular composition and heterotatom variability in OM, particularly the anthropogenically derived variation of DOM, on increased DIC in large rivers remains unknown.

The source and composition of DOM determine the fate of its decomposition, and substantial research has shown that bioavailable, young, and labile OM are preferentially decomposed (Mayorga et al., 2005). The DOM with heteroatomic formulae (dissolved organic nitrogen and sulfur) is preferentially degraded over that without heteroatomic formulae (Vorobev et al., 2018; Hach et al., 2020). An abundance of condensed aromatics, polyphenolics, phenolics from heteroatomic formulae have been shown in samples that appear dominated by stable DOM due to the relative oxygen-enriched environment in river (Vaughn et al., 2021; Zhou et al., 2022; Spencer et al., 2019; Williams et al., 2010). Previous study has verified that the bioavailability of organic nitrogen (livestock and domestic wastewater) accounted for a large proportion of DOM (Zhang et al., 2016a, 2019; Chen et al., 2022a). The dissolved amino acid (one kind of N-containing DOM) can be utilized by phytoplankton directly, promoting the consumption of DOM and production of labile DOM (Zhao et al., 2019; Chen et al., 2021b). High N-containing molecules indicated rich protein-like compounds and tend to be more easily be degraded (Li et al., 2023) besides the aliphatic with high H/C (Zhou et al., 2022). The turnover rate of high lability N-containing DOM is much short and scaled from minutes to hours due to the rapid activities of microorganisms (Zheng et al., 2020). Furthermore, protein-like compounds or metabolized humic-like compounds has been shown to elevate the metabolism of microbes and mineralization of DOM, eventually leading to the release of DIC (Zhou et al., 2022, 2021). Clearly, biolabile DOM in the river would increase the organic-sourced CO_2 and then alter the concentration and source of DIC in a river. Thus, fully understanding the linkage between biolabile DOM and increased DIC in rivers can help to comprehensively understand the genernation of DIC in the riverine and terrestrial-oceanic carbon cycles.

The Yangtze River is the longest river in Asia and a vital channel to export terrestrial carbon to the ocean, and it is estimated that 1502 × 10^9 mol DIC was transported to ocean through this river, the second largest global fluxes of DIC in rivers (Shan et al., 2020; 2021). With the increasing pressure of human activities in the Yangtze River Basin in recent years (Zhou et al., 2021; Meng et al., 2023), it is more and more necessary to study the organic source in the DIC cycle of this river. Therefore, the primary objective of this study was to reveal how variations in the DOM molecular composition may regulate the organic sources of DIC in the Yangtze River. Stable carbon isotopes of DIC, Fourier transform ion cyclotron mass spectrometry (FT-ICR MS), and optical spectroscopy of DOM were performed on samples from the Yangtze River, China to: 1) trace the contribution of organic-sourced DIC, 2) investigate the distribution and variation of DOM, and 3) examine the effect of DOM on organic-sourced DIC.

2. Materials and methods

2.1. Study area and sampling strategy

With a length of approximately 6400 km, the Yangtze River is the longest river in Asia, and its watershed includes the large cities of Chongqing, Wuhan, Nanjing, and Shanghai (Qi et al., 2014; Yang et al., 2014). The Yangtze River Economic Belt is the main artery of the Chinese economy, contributing approximately 46.2 % of China's gross domestic product, and the gross domestic product of the increases gradually along the river continuum, especially in the plain of the middle and lower reaches of the Yangtze River (Zhou et al., 2021; L.Z. Meng et al., 2023). The discharge and sediment concentrations of the Yangtze River show large seasonal variability, with the highest and lowest discharge and sediment concentrations observed in July and December, respectively (Fig. 1). Rainfall is mainly concentrated between May and October, accounting for 70–90 % of the annual rainfall (Zhou et al., 2021; Zhang et al., 2014).

In this study, total of 71 and 115 surface water samples were collected in December 2020 (dry season) and May 2021 (wet season) from Chongqing to Shanghai along the Yangtze River (Fig. 1), for analysis of DIC content and isotopes, optical characteristics of DOM, and other environmental factors. Thereinto, total of 39 samples in the river continuum, 12 in December 2020 and 27 in May 2021, especially in sites near metropolis and rivers confluence, were selected for the DOM molecular characteristics analysis (Fig. 1).

2.2. Content, stable caron isotope, and source of DIC

The total dissolved carbon (TDC) and dissolved organic carbon (DOC) concentrations were measured using a total organic carbon analyser (Shimadzu TOC-L, Japan), and the dissolved inorganic carbon (DIC) concentrations were calculated from the difference between the TDC and DOC (Text S1). After water samples were reacted in a helium ambient sample bottle containing 0.2 ml 85 % phosphoric acid for 6–8 h, stable carbon isotope ratios of DIC ($\delta^{13}C_{DIC}$) were measured using a MAT253 plus isotope ratio mass spectrometer with a Gas Bench II

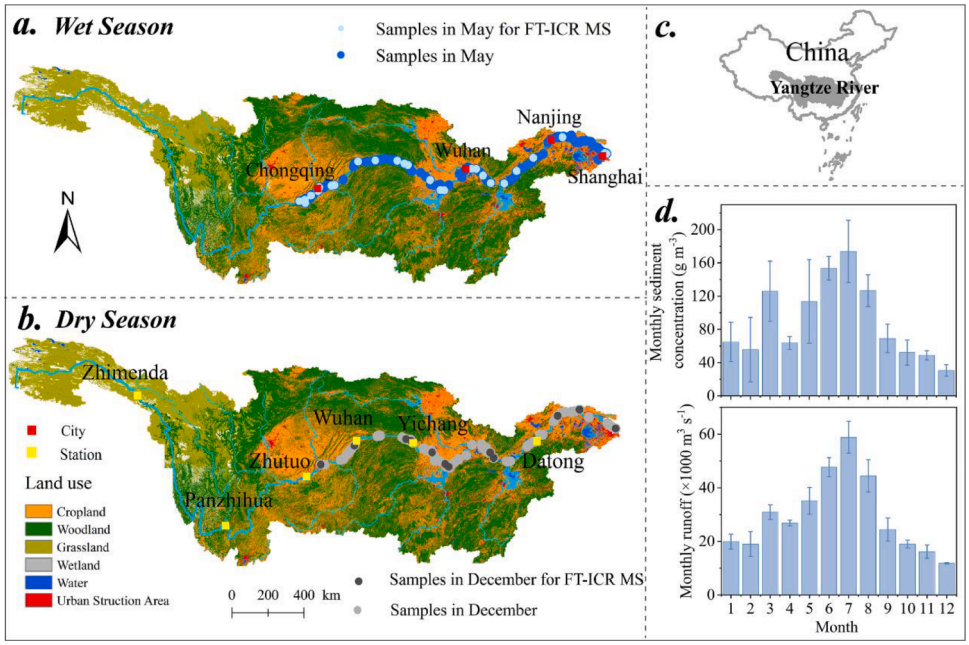

Fig. 1. (a-b) Sampling sites in the Yangtze River during wet season and dry season. (c) Location of the Yangtze River Basin. (d) Seasonality of runoff and sediment concentration for the Datong hydrometric station.

automated device (Thermo Fisher Scientific, USA) (Text S1) (Lang et al., 2011; Li et al., 2022). The results were calibrated against the Vienna Pee Dee Belemnite (V-PDB) standard, and the analytical precisions of $\delta^{13}C_{DIC}$ were 0.15 ‰, respectively.

DIC sources analyses were conducted using Bayesian mixing model in "MixSIAR" package of R 4.0.4, and Bayesian mixing model is based on Markov chain Monte Carlo algorithm to output source probability distribution, which improved accuracy and fault tolerance (Meng et al., 2021). Source of weathering and organic matter were selected as potential sources of DIC in this study, and the end member values was obtained from previous studies and shown in Table S1 (Text S1) (Ishikawa et al., 2015; Telmer and Veizer 1999; Amiotte-Suchet et al., 1999). Based on the Markov Chain Monte Carlo (MCMC) sampling algorithm, the output of the Bayesian model is a probability distribution, and the average value is taken as the source results. Sensitivity analysis of Bayesian mixing model were taken, and the influence of fluctuation in endmember range of 0.2 ‰ on the source result is less than 0.5 %.

2.3. Molecular characteristics of DOM acquired from FT-ICR Ms

DOM from filtered water samples was extracted using PPL cartridges (Agilent) according to the methods of Dittmar et al. (2008). The methanol eluates containing the extracted DOM were analyzed by negative-ion electrospray ionization with a custom-built hybrid linear ion trap FT-ICR MS equipped with a 21 T superconducting solenoid magnet (Hendrickson et al., 2015; Smith et al., 2018). In this study, the number proportion of formulae classified components (CHO%, CHON%, CHOS% and CHONS%) were calculated. The molecular compounds were categorised as highly unsaturated and phenolic-low O/C (HUP-L), highly unsaturated and phenolic-high O/C (HUP-H), Polyphenolic-high O/C (Poly-H), Polyphenolic-low O/C (Poly-L), condensed aromatics (CArom), peptide-like, sugar-like, and aliphatic, and the percentage of the elemental molecules in each molecular compound were determined. In addition, modified aromaticity index (AI_{mod}) and nominal oxidation state of carbon (NOSC) were calculated based on molecular formula (Fig. S1). Detailed information on the FT-ICR MS analyses and molecular calculation methods is provided in Text S1.

2.4. Optical characteristics of DOM, and other chemical analysis

The optical properties of DOM were measured using a UV-3600 spectrophotometer (Shimadzu, Japan) and an FS5 spectrofluorometer (Edinburgh Instruments) after passing through pre-rinsed 0.22 μm Millipore filters. This study provides information on specific ultraviolet absorbance (SUVA254), biological index (BIX), humification index (HIX), and three humic-like components (C1-C3) and two protein-like components (C4-C5) was well validated by Parallel factor analysis (PARAFAC) (Table S2). The calculation and model used for these properties can be found in Text S1, and the variation of the five components, BIX, and SUVA254 are shown in Figs S2 and S3.

$\delta^{13}C_{DOC}$ was determined by persulfate wet oxidation and thermal methods (Lang et al., 2011). The water sample in the bottle reacts with hydrochloric acid to remove the inorganic carbon and is filled with helium gas, and then the headspace carbon dioxide is generated after the action of oxidizing agent during 100 °C and measured by MAT253 plus isotope ratio mass spectrometer with a Gas Bench II automated device (Thermo Fisher Science, Bremen, Germany). $\delta^{13}C_{CO2}$ was measured using a Picarro G2131-i with a small sample introduction module (Picarro A0314 SSIM) (Miller et al., 2022), and the $\delta^{2}H$ and $\delta^{18}O$ values of the water samples were measured using an L2130-i High Accuracy Water Isotope Analyzer (Picarro, USA) (Wu et al., 2018). The concentrations of total dissolved nitrogen (TDN), ammonium (NH_4^+), and nitrate (NO_3^-) in the water samples were determined using the potassium persulfate digestion and spectrophotometric method, the nesslerization colorimetric method, and phenol disulfonic acid ultraviolet spectrophotometric method (Chen et al., 2022b), water temperature, SpC, and pH in the water samples were determined according to previous studies (Text S1) (Jin and Tu 1990).

2.5. Redundancy analysis

Redundancy analysis (RDA) was conducted to evaluate the impact of the DOM source and environmental factors on organic-sourced DIC. Optical properties indexes of DOM, source ($\delta^{13}C_{DOC}$), temperature, pH, nutrients and $\delta^{13}C_{DIC}$, and organic-sourced DIC in the wet and dry seasons were adopted to conduct RDA analysis.

3. Results

3.1. Content, stable carbon isotopic and organic-source contribution of DIC

The DIC concentrations obtained from the Yangtze River ranged from 1619 μmol L^{-1} to 2497 μmol L^{-1} with mean values of 2016±288 μmol L^{-1} and 2120±143 μmol L^{-1} in wet and dry seasons, respectively, and showed a decreasing trend from upstream to downstream (Fig. 2). Spatially, $\delta^{13}C_{DIC}$ was much more enriched in upstream, and more depleted in downstream, with the highest values of −6.4 ‰ and −6.2 ‰ in wet and dry seasons, respectively, and the lowest values of −9.7 ‰ and −9.2 ‰ in wet and dry seasons, respectively. Seasonally, the $\delta^{13}C_{DIC}$ in wet season (mean value, −8.5 ± 1.0 ‰) was more depleted than that in dry season (mean value, −8.0 ± 0.8 ‰). Correspondingly, the contribution of organic-sourced DIC (DIC_{OC}) increased from upstream to the estuary, according to the analysis of Bayesian mixing models. The percentage of DIC_{OC} was much lower in upstream (approximately 17.4 %) than in downstream (approximately 50.4 %). The DIC_{OC} in wet season (40.0 ± 12.1 %) was higher than that in dry season (32.0 ± 7.2 %).

3.2. Molecular formula composition of DOM

The number of assigned DOM formulae in the Yangtze River ranged from 7967 to 16,752, and the DOM formulae in wet season (with an average of 15,087±956) was greater than that in dry season (with an average of 12,713±1898) (Fig. 3). CHO accounted for 39.12±2.69 % of DOM, and showed a decreasing trend along the river with a percentage range of 35.15~41.00 % and 36.79~48.81 % in wet and dry season, respectively (Fig. 3 and Table S3). As for heteroatomic compound DOM, CHON was the dominant component, accounting for 41.77±2.55 % of DOM, and fluctuatedly increased with an range of 38.59~47.39 % and 33.81~44.54 % from upstream to downstream in wet and dry season, respectively (Fig. 3 and Table S3). CHOS only accounted for 14.64 ±1.73 % of DOM, and the percentage showed a decreasing trend along the river, with an range of 9.64~17.47 % and 11.18~16.38 % in wet and dry season, respectively (Fig. 3 and Table S3). CHONS was the smallest contributor to the DOM, only accounting for 4.95±0.82 % and 3.40±1.02 % in wet and dry season, respectively, and gradually increases along the river continuum (Fig. 3 and Table S3).

3.3. Molecular composition in different classified compound categories

Seven classified compound categories were recognized in this study, and the distribution patterns of compound categories were silimar in wet and dry seasons (Fig. 4 and Table S4). Highly unsaturated and phenolic compounds (HUP) were the dominant components, accounting for 81.89~88.38 % of DOM, among which the percentage of highly unsaturated and phenolic compounds with high O/C (HUP-H) accounting for 32.66~41.93 %, and the highly unsaturated and phenolic compounds containing low O/C (HUP-L) accounting for 42.58~53.09 % (Fig. 4 and Table S4). Polyphenolics (Poly) were the second principal component, with a percentage of 9.35±1.24 %, polyphenolics with high O/C (Poly-H) and low O/C (Poly-L) accounted 2.67~4.73 % and 4.21~8.13 %, respectively (Fig. 4 and Table S4). The proportions of condensed aromatics (CArom), sugar-like compounds, and peptide-like compounds were much lower, with the rang of 0.67~2.25 %, 0.42~2.44 % and 0.76~6.28 %, respectively (Fig. 4 and Table S4).

Similar to the molecular composition of DOM, CHO and CHON were dominated in different formulae-classified compound categories, and the proportion of CHOS and CHONS were lower (Fig. 4 and Table S5). Similar patterns of molecular composition were found in HUP in wet and dry seasons, and HUP (including HUP-H and HUP-L) presented obvious CHO and CHON dominance. The average percentage of CHON in HUP-H and HUP-L was 38.41~48.18 % and 36.09~54.43 %, respectively (Fig. 4 and Table S5), and CHO accounted for 33.02~48.32 % and 33.96~49.46 % in HUP-H and HUP-L, respectively (Fig. 4 and Table S5). Molecular composition of Poly (including Poly-H and Poly-L) and CArom showed seasonal differences. In wet season, CHO was the mainly company in Poly and CArom, with a ranged of 44.48~57.70 %, 40.29~64.71 % and 63.16~77.91 % in Poly-H, Poly-L and CArom, respectively. Followed by CHON, the percentage range of CHON in Poly-H, Poly-L and CArom were 41.97~48.42 %, 30.58~46.53 % and 11.84~34.97 %, respectively. In dry season, the molecular composition of Poly-H is similar to wet season, but the percentage of CHOS in Poly-L and CArom obviously higher than that in wet season. CHOS, accounting for 44.03±6.90 % in Poly-L, was the main composition, followed by CHO and CHON, accounting for 29.66±3.07 % and 23.53±6.02 % in Poly-L, respectively. CHO was the primarily component of CArom with a percentage of 49.80±8.64 %, and CHOS was secondary component with a porprotion of 39.65±12.94 %. As for Suger and Petide-like, CHON showed obvious dominance both in wet and dry season, with percentage range of 44.44~100.00 % and 69.29~100.00 % in Suger and Petide-like, respectively. Specially, a increasing trend from upstream to downstream were observed in the percentage of CHON in HUP-L, Poly-H, Poly-L and CArom and the percentage of CHONS in HUP-H, HUP-L, Poly-H, and the other molecular composition percentage decreased or fluctuated along the river continuum (Fig. 4).

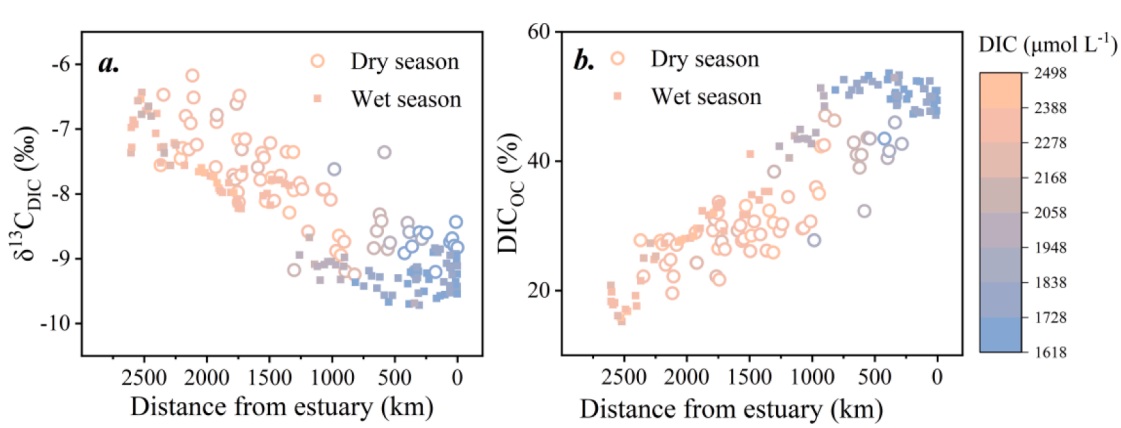

Fig. 2. Variation of $\delta^{13}C_{DIC}$ (a) and the percentage of organic-sourced DIC (b) with the variation of DIC concentration in the Yangtze River during dry (December) and wet (May) seasons.

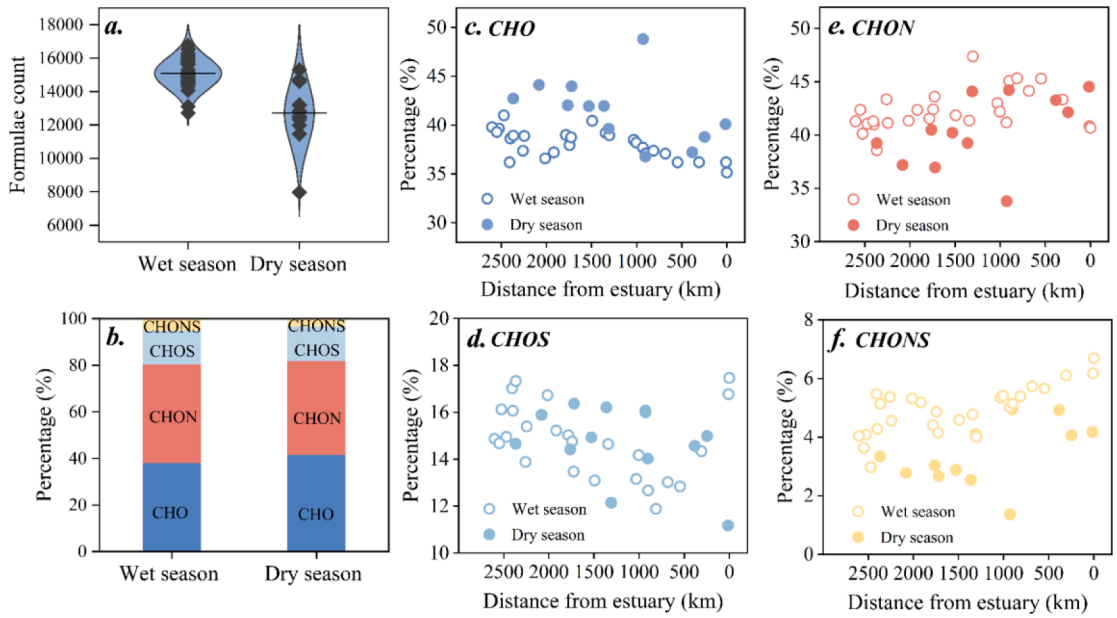

Fig. 3. (a) Formulae count of DOM in the Yangtze River in wet and dry season. (b) Percentage of CHO, CHOS, CHON and CHONS molecular formula in DOM of the Yangtze River in wet and dry season. (c-f) Variation of CHO, CHOS, CHON and CHONS percentage along the Yangtze River during wet and dry season.

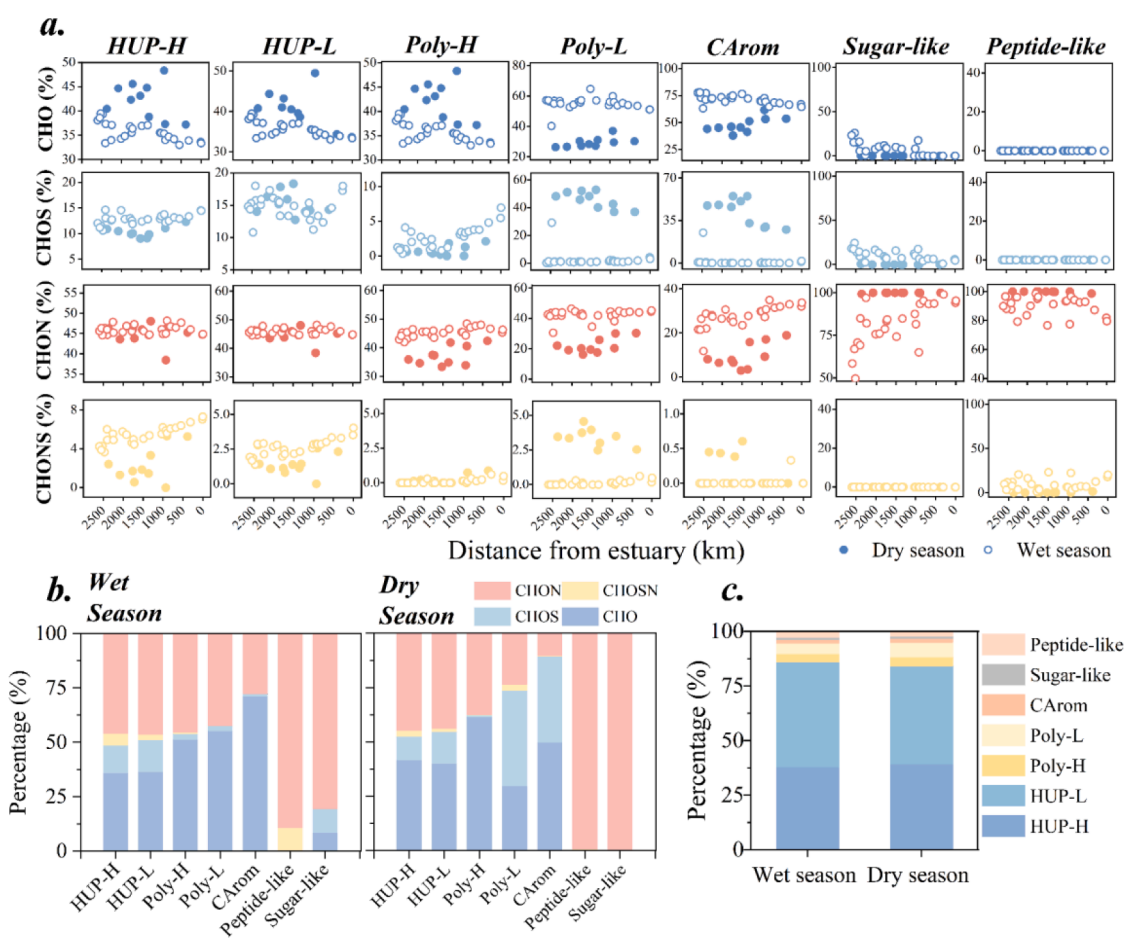

Fig. 4. (a) The variation of CHO, CHON, CHOS and CHONS contribution in formulae classified components along the Yangtze river during wet and dry season. (b) The percentage of CHO, CHON, CHOS, and CHONS in the formulae classified components of the Yangtze River. (c) The percentage of formulae classified components in the Yangtze River (highly unsaturated and phenolic-high O/C (HUP-H), highly unsaturated and phenolic-low O/C (HUP-L), polyphenolic-high O/C (Poly-H), Polyphenolic-low O/C (Poly-L), Condensed aromatics (CArom), Peptide-like and Sugar-like).

4. Discussion

4.1. Higher oxidation state of N-containing DOM in the Yangtze river

Organic compounds with different DOM molecular formula have different utilization potential of microbial and photodegradation (Gonsior et al., 2011; Riedel et al., 2016; Hu et al., 2022). Enriching heteroatomic formulae has been proved can alter the reactivity of DOM, and the high lability DOM with heteroatomic formulae is preferentially degraded (Wagner et al., 2015; Vorobev et al., 2018; Hach et al., 2020). For the Yangtze River, nitrogen containing molecule is the dominant component of DOM, and CHON accounted for approximately 40 % of DOM (Fig. 3). Compared with other majore rivers, the percentage of CHON in the Yangtze River also apparently higher than that in Suwannee, Kissimmee, Mississippi and Amazon rivers (Table S6). Previous studies revealing that human activities and associated land use cover change increase the nitrogen formulae content, sucn as forest DOM presented a significant abundance of CHO, while agricultural DOM showed more N-containing formulae (CHON) (Vaughn et al., 2021; Spencer et al., 2019; Drake et al., 2019a b; Kurek et al., 2020; 2022). The superior CHON in the Yangtze River than other regions may caused by the higher intensity of anthropogenic influence in the river basin than that in forest-dominated catchments.

Oxidation state is an important indicator of DOM degradation potential, and thermodynamically, highly oxidised DOM molecules are preferentially degraded, and reduced DOM molecules tend to persist in aquatic systems (Kellerman et al., 2015; Boye et al., 2017). The nominal oxidation state of carbon (NOSC), which characterises the oxidation state of carbon, is a thermodynamic indicator of biodegradability (LaRowe and Cappellen 2011; Chen et al., 2022c). For the Yangtze River, the average NOSC was −0.17±0.03, which is contisitant with lignin-like substance (from −0.2 to −0.1). The average NOSC values of CHON and CHONS were 0.14±0.18 and 0.17±0.10, respectively, which is obvious higher than that of CHO and CHOS (with an average of −0.16 ±0.24 and −0.16±0.11) (Fig. 5). Significant higher NOSC of N-containing DOM molecule category in this river (−0.33 to 0.59) than non N-containing DOM molecule category (−0.76 to 0.39) (Fig. S4) is consistent with previous study (Chen et al., 2022c), which suggested that the presence of nitrogen could potentially improve the degradability of DOM (Boye et al., 2017). Although the NOSC in the Yangtze River has a narrower range compared to those from plant litters (Gunina and Kuzyakov 2022), sediments (Zhou et al., 2019), and soil organic matter (Boye et al., 2017), DOM with a relatively high NOSC induced by N-containing components is expected to have a higher energy content and is more likely to be degraded in the Yangtze River (LaRowe and Cappellen 2011).

4.2. Coupling between N-containing DOM and organic-sourced DIC

The composition of DOM determines the fate of its decomposition, and regulates the generation of DIC_{OC} (Mayorga et al., 2005). The relationships between different DOM molecular composition (CHO, CHON, CHOS, CHONS) and DIC_{OC} were discussed in this study. Our results showed that CHON% ($r = 0.33$, $p < 0.05$) and CHONS% ($r = 0.52$, $p < 0.05$), both with N atoms, were significant positive correlated with DIC_{OC}; while CHO% ($r = -0.34$, $p < 0.05$) and CHOS% ($r = -0.32$, $p < 0.05$), both without N atoms, were significant negative correlated with DIC_{OC} (Fig. 6). The positive relationship between DIC_{OC} and N-containing DOM ($r = 0.43$, $p < 0.05$, Fig. S5) suggests that nitrogen atoms promoted the effect of DOM on DIC_{OC}. Moreover, N/C_{wa} showed a significant positive relationship with DIC_{OC}, also indicating that the present of N atoms promoted the transformation of DOM to DIC_{OC} (the high

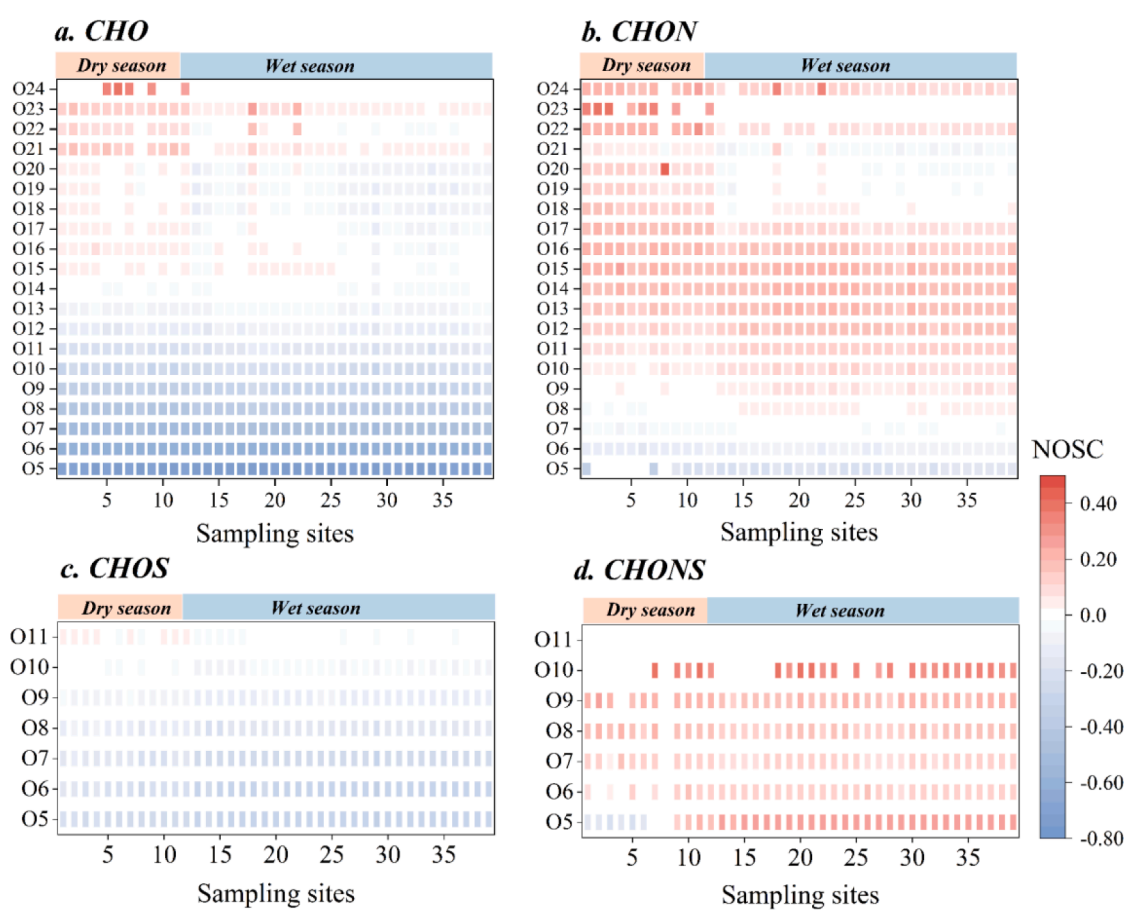

Fig. 5. Nominal oxidation state of carbon (NOSC) of DOM composed different molecular formulas (a. CHO, b. CHON, c. CHOS, d. CHONS).

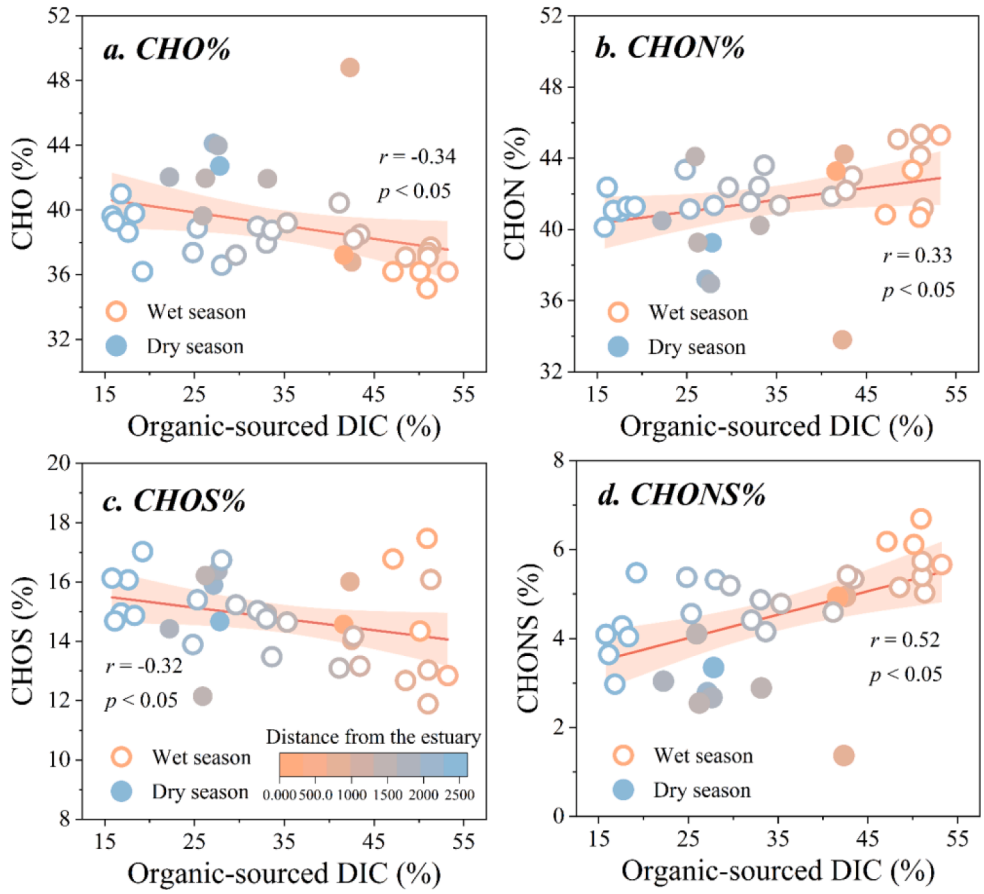

Fig. 6. The relationship between organic-sourced DIC and DOM composed different molecular formulas (a. CHO%, b. CHON%, c. CHOS%, d. CHONS%) in the Yangtze River.

N/C_{wa} is associated with depleted $\delta^{13}C_{DIC}$, as shown in Fig. S6). This finding corfirms the notion that degradation of N-containing DOM may elevate the contribution of DIC_{OC} in river (Drake et al., 2019a).

Furthermore, we conducted a Spearman's rank correlations to reveal the promoting effect of N-containing compound groups on the production of DIC_{OC}. Previous studies have showed that river neworks flowing through urban and agricultural areas transport quantities of anthropogenic DOM, particularly N-containing DOM (Vaughn et al., 2021; Zhou et al., 2022; Spencer et al., 2019; Williams et al., 2010). When comparing the thousands of molecular formular assigned in DOM from the Yangtze River with N atoms and without N atmos, a number of formulae with relative high H/C ratio, such as CHO and CHOS, and low H/C and O/C ratio N- containing formulae, such as CHON and CHONS were found to be significant positively correlated with DIC_{OC} (Fig. 7). Due to their high H/C ratios (% aliphatic) and amine content, these compounds are generally energy-rich and biolabile, and are preferentially decomposed by bacteria over short timeframes (Spencer et al., 2015; Drake et al., 2015), wich is similar to that found in other study areas (Drake et al., 2018; Rossel et al., 2013). The significantly negative Spearman correlation coefficients between the CHO, CHON molecules and DIC_{OC} were predominantly in high O/C and low H/C formulae (Fig. 7), which were specified as forest-derived DOM and inert to be degraded by bacteria (Drake et al., 2019a). In addition, it was found that most aliphatic and HUP in CHOS molecules were positively correlated with DIC_{OC}, Poly in CHOS molecules was negatively correlated with DICoc, and mostly HUP in CHONS molecules were positively correlated with DICoc (Fig. 7). Sewage treatment effluent is a main source of CHOS formulae in river water column (Ye et al., 2019), and the surfactant-like O_3S and O_5S formulae enriched in sewage effluent (Ye et al., 2019) were highly correlated with aliphatic compounds ($r = 0.84$), indicating that the presence of S atoms could also promote DIC_{OC} from DOM. Comparied with dry season, higher percentage of DOM formulaes (CHO, CHON, CHOS, CHONS) were positive correlated with DIC_{OC} in wet season (Fig. 7), which shows that DOM in the dry season is resistant to degradation by DIC_{OC} (Kramer et al., 2004; Jones et al., 2020; Chu et al., 2022).

4.3. Effect of other regulation and driver factors

Degradation of DOM was also regulated by its sources and environmental factors such as temperature, pH, and nutrients (Hu et al., 2022; Koch and Dittmar 2006; Davidson and Janssens 2006). Redundancy analysis (RDA) showed that the concentration of DIC_{OC} ($C_{DIC—OC}$) in wet and dry seasons were both significantly positively related with DOM composition (fluorescent components, C1-C5), source ($\delta^{13}C_{DOC}$), and aromaticity ($SUVA_{254}$) (Fig. 8). Seasonal environmental factors have different effects on DIC_{OC}. The influence of BIX, affected by temperatures, on DIC_{OC} in wet season is stronger than that in dry season. pH, NH^{4+} and Spc had significant negative effects on DIC_{OC} in the wet season, while pH had significant positive effects on DIC_{OC} in the dry season (Fig. 8).

DIC_{OC} was found to be associated with more aromatic/terrestrial inputs, which reflecting in the Spearman correlation between $SUVA_{254}$, $\delta^{13}C_{DOC}$ and molecular formulae (Fig. S7 and S8) (Rossel et al., 2013; Mesfioui et al., 2015; Qiao et al., 2021). Soil erosion caused by high rainfall during the wet season may push more DIC from soil organic matter into river. The strong relationship between $C_{DIC—OC}$ and humic-like components (C1-C3) in wet season also further confirmed the aromaticity of allochthonous DOM, whereas protein-like components (C4-C5) and part of humic-like components (C1) were correlated with

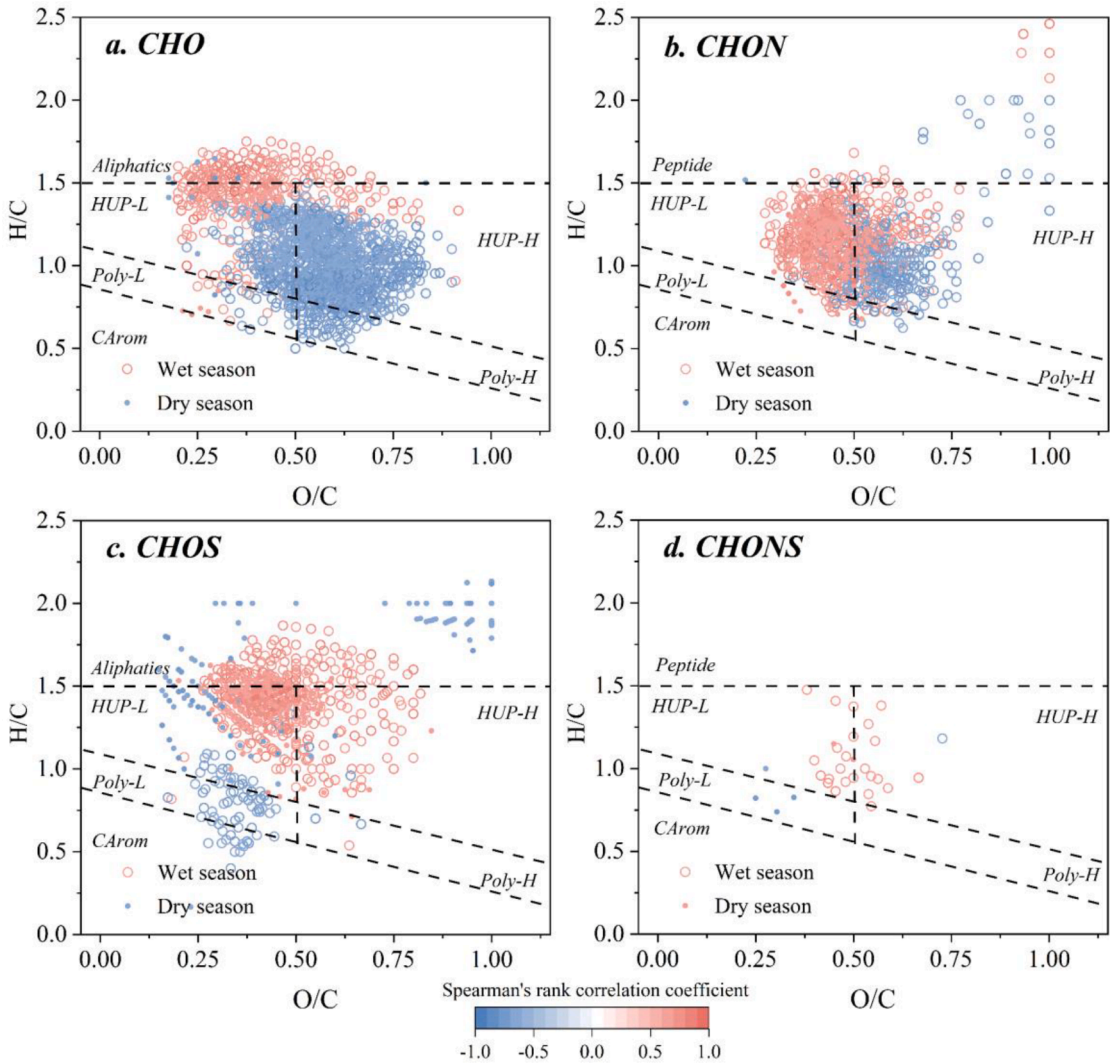

Fig. 7. Spearman's rank correlations of (a) CHO, (b) CHON, (c) CHOS and (d) CHONS percentage of DOM with organic-sourced DIC ($p<0.05$). Colors represent the Spearman correlation coefficient between each molecular formula and organic-sourced DIC, solid and hollow circle represent dry and wet seasons, respectively.

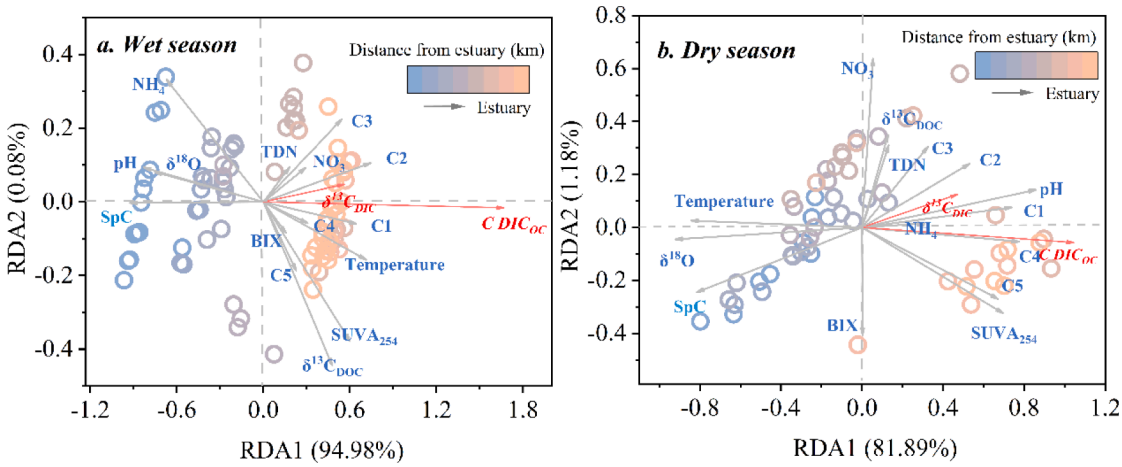

Fig. 8. Redundancy analysis (RDA) of other regulation and driver factors on concentration of DIC_{OC} and $\delta^{13}DIC$ in wet (a) and dry (b) seasons. The circle colours represent the samples from upstream to downstream.

the $C_{DIC—OC}$ in dry season (Fig. 8). The N/C_{wa}, temperature, and humic-like components (C3) significantly regulate the $C_{DIC—OC}$ with a relatively high correlation, and the percentage of $C_{DIC—OC}$ to DIC ($\delta^{13}C_{DIC}$) is dominated by DON, NO_3^-, S/Cwa, aliphatic and N/C_{wa} for all data in wet and dry seasons (Fig. S9). The stable carbon isotopes of DIC, DOC, and CO_2 also demonstrate that upstream weathering mainly

consumes atmospheric CO_2, and human activities raised the allochthonous DOM and then elevated the respiration DIC_{OC} (Fig. S10) (Mackensen and Schmiedl 2019).

The correlations among different molecular, isotopic, and optical parameters would facilitate the understanding of the effect of DOM composition and source on DIC_{OC} (Fig. S11). The significant positive correlations between the molecular ratios (S/Cwa, N/C_{wa}) and absorption coefficient ($a254$) (DOC is highly correlated to $a254$) suggest that N- and S-containing and synchronous DOM dominated DOC in the Yangtze River. H/C exhibited a high correlation with the five fluorescence components in the dry season (mean $r = 0.77$) and almost no correlation in the wet season. Molecular CHON and CHONS were mainly distributed in C4 (tryptophan-like), particularly during the wet season ($r = 0.45$ and 0.56). The significant negative correlations between AImod and marine humic-like (C1) ($r = -0.86$) and the positive correlation between AImod and $\delta^{13}C_{DOC}$ in dry season ($r = 0.46$) suggested that autochthonous humic-like components increase the AImod in the Yangtze River, which is different from previous studies on boreal and coastal waters (Stubbins et al., 2014; Sun et al., 2022).

5. Conclusion

Our research revealed that organic matter degradation is a crucial source of DIC in the Yangtze River, accounting for 40.0 ± 12.1 % and 32.0 ± 7.2 % of DIC in wet and dry seasons, respectively, and increasing along the river by approximately three times. Nitrogen-containing DOM is an important composition in DOM, with a percentage of ~40 %. Superior oxidation state of nitrogen-containing DOM than non nitrogen-containing DOM and positive relationship between DIC_{OC} and N-containing DOM formulae both suggested that the presence of nitrogen could improve the degradable potential of DOM. Moreover, molecular formular with low H/C and O/C ratio N-containg formulae were positively correlated with DIC_{OC} further verified these energy-rich and biolabile compounds are preferentially decomposed by bacteria to produce DIC. Overall, our study revealed that N-containing components significantly elevated the oxidation state of DOM and promoted its effect on organic-sourced DIC, which is of vital significance to understand the environmental process of DIC, CO_2 emission and even carbon cycling in large rivers.

Declaration of Competing Interest

The authors declare that they have no known competing financial interests or personal relationships that could have appeared to influence the work reported in this paper.

Data availability

Data will be made available on request.

Acknowledgement

This study was supported by grants from the National Natural Science Foundation of China (No. 42277214, 42207256, and 41971286), major programs of the National Social Science Foundation of China (Grant No. 22&ZD136), the Special Science and Technology Innovation Program for Carbon Peak and Carbon Neutralization of Jiangsu Province (Grant No. BE2022612), the Youth Top Talent funded by Nanjing Normal University, China Postdoctoral Science Foundation Funded Project (Grant No. 2022M721661), the Open Fund of the State Key Laboratory of Lakes and Environment (2022SKL019), and the Postgraduate Research & Practice Innovation Program of Jiangsu Province (Grant No. KYCX23_1701). The Ion Cyclotron Resonance user facility at the National High Magnetic Field Laboratory at Florida State University was supported by the National Science Foundation Division of Materials Research and Division of Chemistry through DMR 16–44779, and the State of Florida.

Supplementary materials

Supplementary material associated with this article can be found, in the online version, at doi:10.1016/j.watres.2023.120808.

References

Amiotte-Suchet, P., Aubert, D., Probst, J.L., Gauthier-Lafaye, F., Probst, A., Andreux, F., Viville, D., 1999. $\delta^{13}C$ pattern of dissolved inorganic carbon in a small granitic catchment: the Strengbach case study (Vosges mountains, France). Chem. Geol. 159, 129–145.

Appling, A.P., Read, J.S., Winslow, L.A., Arroita, M., Bernhardt, E.S., Griffiths, N.A., Hall Jr, R.O., Harvey, J.W., Heffernan, J.B., Stanley, E.H., Stets, E.G., Yackulic, C.B., 2018. The metabolic regimes of 356 rivers in the United States. Scient. Data. 5, 180292.

Aufdenkampe, A.K., Mayorga, E., Raymond, P.A., Melack, J.M., Doney, S.C., Alin, S.R., Aalto, R.E., Yoo, K., 2011. Riverine coupling of biogeochemical cycles between land, oceans, and atmosphere. Front. Ecol. Environ 9, 53–60.

Battin, T.J., Kaplan, L.A., Findlay, S., Hopkinson, C.S., Marti, E., Packman, A.I., Newbold, J.D., Sabater, F., 2008. Biophysical controls on organic carbon fluxes in fluvial networks. Nat. Geosci 1, 95–100.

Battin, T.J., Ronny, L., Emily, S.B., Enrico, B., Lluís, G.G., Robert, O.H.J., Erin, R.H., Taylor, M., Tamlin, M., Pavelsky, L.R., Peter, R., Judith, A., Rosentreter, P.R., 2023. River ecosystem metabolism and carbon biogeochemistry in a changing world. Nature 613, 449–459.

Bernhardta, E.S., Savoy, P., Vlah, M.J., Appling, A.P., Koenig, L.E., Hall Jr., R.O., Arroita, M., Blaszczak, J.R., Carter, A.M., Cohen, M., Harvey, W.J., Heffernan, J.B., Helton, A.M., Hosen, J.D., Kirk, L., McDowell, W.H., Stanley, E.H., Yackulic, C.B., Grimm, N.B., 2022. Light and flow regimes regulate the metabolism of rivers. Proc. Natl. Acad. Sci. U.S.A. 119, e2121976119.

Boye, K., Noël, V., Tfaily, M.M., Bone, S.E., Williams, K.H., Bargar, J.R., Fendorf, S., 2017. Thermodynamically controlled preservation of organic carbon in floodplains. Nat. Geosci 10, 415–421.

Cai, W.J., 2011. Estuarine and coastal ocean carbon paradox: CO_2 sinks or sites of terrestrial carbon incineration. Ann. Rev. Mar. Sci 3, 123–145.

Chen, H., Selim Ersan, M.S., Tolicd, N., Chu, R.K., Karanfil, T., Chow, A.T., 2022c. Chemical characterization of dissolved organic matter as disinfection byproduct precursors by UV/fluorescence and ESI FT-ICR MS after smoldering combustion of leaf needles and woody trunks of pine (Pinus jeffreyi). Water Res. 209, 117–962.

Chen, Q., Chen, F., Gonsior, M., Li, Y.Y., Wang, Y., He, C., Cai, R.H., Xu, J.X., Wang, Y.M., Xu, D.P., Sun, J., Zhang, T., Shi, Q., Jiao, N.Z., Zheng, Q., 2021b. Correspondence between DOM molecules and microbial community in a subtropical coastal estuary on a spatiotemporal scale. Environ. Int 154, 106558.

Chen, S., Zhong, J., Li, C., Liu, J., Wang, W.F., Xu, S., Li, S.L., 2021a. Coupled effects of hydrology and temperature on temporal dynamics of dissolved carbon in the Min River. Tibetan Plateau. J. Hydrol. 593, 125641.

Chen, X.J., Wang, M.R., Kroeze, C., Chen, X., Ma, L., Chen, X.P., Shi, X.J., Strokal, M., 2022a. Nitrogen in the Yangtze River Basin: pollution reduction through coupling crop and livestock production. Environ. Sci. Technol. 56 (24), 17591–17603.

Chen, Z.L., Huang, X.H., Huang, C.C., Yang, Y.J., Yang, H., Zhang, J.B., Huang, T., 2022b. High atmospheric wet nitrogen deposition and major sources in two cities of Yangtze River Delta: combustion-related NH3 and non-fossil fuel NOx. Sci. Total Environ 806, 150502.

Chu, J.Y., Luo, C.J., Wang, H.J., Liao, Z.L., 2022. Insights into the associations between optical and molecular signatures of dissolved organic matter from urban stormwater runoff. ACS ES&T Water 2, 339–348.

Cole, J.J., Prairie, Y.T., Caraco, N.F., McDowell, W.H., Tranvik, L.J., Striegl, R.G., Duarte, C.M., Kortelainen, P., Downing, J.A., Middelburg, J.J., Melack, J.M., 2007. Plumbing the global carbon cycle: integrating inland waters into the terrestrial carbon budget. Ecosystems 10, 171–184.

Davidson, E.A., Janssens, I.A., 2006. Temperature sensitivity of soil carbon decomposition and feedbacks to climate change. Nature 440, 165–173.

Dittmar, T., Koch, B., Hertkorn, N., Kattner, G.A., 2008. Simple and efficient method for the solid-phase extraction of dissolved organic matter (SPE-DOM) from seawater. Limnol. Oceanog. 6, 230–235.

Drake, T.W., Guillemette, F., Hemingway, J.D., Chanton, J.P., Podgorski, D.C., Zimov, N. S., Spencer, R.G.M., 2018. The ephemeral sig-nature of permafrost carbon in an arctic fluvial network. J. Geophy. Res. 123 (5), 1475–1485.

Drake, T.W., Podgorski, D.C., Dinga, B., Chanton, G.P., Six, J., Spencer, R.G.M., 2019a. Land-use controls on carbon biogeochemistry in lowland streams of the Congo Basin. Glob. Chang. Biol 26, 1374–1389.

Drake, T.W., Van Oost, K., Barthel, M., Bauters, M., Hoyt, A.M., Podgorski, D.C., Spencer, R.G.M., 2019b. Mobilization of aged and biolabile soil carbon by tropical deforestation. Nat. Geosci 12, 541–546.

Drake, T.W., Wickland, K.P., Spencer, R.G.M., McKnight, D.M., Striegl, R.G., 2015. Ancient low–molecular-weight organic acids in permafrost fuel rapid carbon dioxide production upon thaw. Proceed. Nat. Acad. Sci. 112 (45), 13946–13951.

Gonsior, M., Zwartjes, M., Cooper, W.J., Song, W.H., Ishida, K.P., Tseng, L.Y., Jeung, M. K., Rosso, D., Hertkorn, N., Schmitt-Kopplin, P., 2011. Molecular characterization of

effluent organic matter identified by ultrahigh resolution mass spectrometry. Water Res. 45, 2943–2953.
Gounand, I., Little, C.J., Harvey, E., Altermatt, F., 2018. Cross-ecosystem carbon flows connecting ecosystems worldwide. Nat. Commun 9, 4825.
Gunina, A., Kuzyakov, Y., 2022. From energy to (soil organic) matter. Glob. Chang. Biol 28, 2169–2182.
Hach, P.f., Marchant, H.K., Krupke, A., Riedel, T., V., Meier, D., Lavik, G., Holtappels, M., Dittmar, T., Kuypers, M.M.M., 2020. Rapid microbial diversifcation of dissolved organic matter in oceanic surface waters leads to carbon sequestration. Sci. Rep 10, 13025.
Hendrickson, C.L., Quinn, J.P., Kaiser, N.K., Smith, D.F., Blakney, G.T., Chen, T., Marshall, A.G., Weisbrod, C.R., Beu, S.C., 2015. 21 Tesla Fourier transform ion cyclotron resonance mass spectrometer: a national resource for ultrahigh resolution mass analysis. J. Am. Soc. Mass Spectrom. 26, 1626–1632.
Herath, I.K., Wu, S.J., Ma, M.H., Ping, H., 2022. Dynamic of riverine pCO_2, biogeochemical characteristics, and carbon sources inferred from δ13C in a subtropical river system. Sci. Total Environ 821, 153–296.
Hu, A., Jang, K., Meng, F.F., Stegen, J., Tanentzap, A.J., Choi, M., Lennon, J.T., Soininen, J., Wang, J.J., 2022. Microbial and environmental processes shape the link between organic matter functional traits and composition. Environ. Sci. Technol. 56, 10504–10516.
Huang, T.H., Fu, Y.H., Pan, P.Y., Chen, C.T.A., 2012. Fluvial carbon fluxes in tropical rivers. Curr. Opin. Environ. Sustain 4, 162–169.
Ishikawa, N.F., Tayasu, I., Yamane, M., Yokoyama, Y., Sakai, S., Ohkouchi, N., 2015. Sources of dissolved inorganic carbon in two small streams with different bedrock geology: insights from carbon isotopes. Radiocarbon 57, 439–448.
Jin, X., Tu, Q., 1990. The Stand Methods For Observation and Analysis in Lake Eutrophication. Chinese Environmental Science Press, Beijing.
Jones, M.W., Coppola, A.I., Santín, C., Dittmar, T., Jaffé, R., Doerr, S.H., Quine, T.A., 2020. Fires prime terrestrial organic carbon for riverine export to the global oceans. Nat. Commun 11, 27–91.
Kaushal, S.S., Likens, G.E., Utz, R.M., Pace, M.L., Grese, M., Yepsen, M., 2013. Increased river alkalinization in the Eastern US. Environ. Sci. Technol. 47, 10302–10311.
Kellerman, A.M., Kothawala, D.N., Dittmar, T., Tranvik, L.J., 2015. Persistence of dissolved organic matter in lakes related to its molecular characteristics. Nat. Geosci 8, 454–457.
Koch, B.P., Dittmar, T., 2006. From mass to structure: an aromaticity index for high-resolution mass data of natural organic matter. Rapid Comm. Mass Spectro. 20, 926–932.
Köhler, P., Hartmann, J., Wolf-Gladrowa, D.A., 2010. Geoengineering potential of artificially enhanced silicate weathering of olivine. Proc. Natl. Acad. Sci. U.S.A. 107, 20228–20233.
Kramer, R.W., Kujawinski, E.B., Hatcher, P., 2004. Identification of Black Carbon Derived structures in a volcanic ash soil humic acid by fourier transform ion cyclotron resonance mass spectrometry. Environ. Sci. Technol. 38, 3387–3395.
Kurek, M.R., Poulin, B.A., McKenna, A.M., Spencer, R.G., 2020. Deciphering dissolved organic matter: ionization, dopant, and fragmen-tation insights via Fourier transform-ion cyclotron resonance mass spectrometry. Environ. Sci. Technol. 54, 16249–16259.
Kurek, M.R., Stubbins, A., Drake, T.W., Dittmar, T., Moura, J.M.S., Holmes, R.M., Osterholz, H., Six, J., Wabakanghanzi, J.N., Dinga, B., Mitsuya, M., Spencer, R.G.M., 2022. Organic molecular signatures of the Congo River and comparison to the Amazon. Global Biogeochem. Cycles 36, e2022GB007301.
Lang, S.Q., Bernasconi, S.M., Früh-Green, G.L., 2011. Stable isotope analysis of organic carbon in small (μg C) samples and dissolved organic matter using a GasBench preparation device. Rapid Comm. Mass Spectro 26 (1), 9–16.
LaRowe, D.E., Cappellen, P.V., 2011. Degradation of natural organic matter: a thermodynamic analysis. Geochim. Cosmochim. Acta 75, 2030–2042.
Li, H.M., Feng, X.T., Xiong, T.Q., He, C., Wu, W.C., Shi, Q., Jiao, N.Z., Zhang, Y.Y., 2023. Green tides significantly alter the molecular composition and properties of coastal DOC and perform dissolved Carbon sequestration. Environ. Sci. Technol. 57, 770–779.
Li, J., Pu, J., Zhang, T., 2022. Transport and transformation of dissolved inorganic carbon in a subtropical groundwater-fed reservoir, south China. Water Res. 209, 117905.
Mackensen, A., Schmiedl, G., 2019. Stable carbon isotopes in paleoceanography: atmosphere, oceans, and sediments. Earth-Sci. Rev 197, 102–893.
Martin, J.B., 2017. Carbonate minerals in the global carbon cycle. Chem. Geol. 449, 58–72.
Marzolf, N.S., Ardón, M., 2021. Ecosystem metabolism in tropical streams and rivers: a review and synthesis. Limnol. Oceanogr. 66, 1627–1638.
Mayorga, E., Aufdenkampe, A.K., Masiello, C.A., Krusche, A.V., Hedges, J.I., Quay, P.D., Richey, J.E., Brown, T.A., 2005. Young organic matter as a source of carbon dioxide outgassing from Amazonian rivers. Nature 436, 538–541.
Meng, L., Hao, W.Y., Zhao, C., Li, S.D., Xue, J.Y., Li, J.H., Tu, L.Y., Huang, T., Yu, Z.Y., Yuan, L.Y., Huang, C.C., 2023a. Anthropogenic activities generate high-refractory Black Carbon along the Yangtze River continuum. Environ. Sci. Technol. 57, 8598–8609.
Meng, L., Zhao, Z., Lu, L., Zhou, J., Luo, D., Fan, R., Li, S., Jiang, Q., Huang, T., Yang, H., Huang, C., 2021. Source identification of particulate organic carbon using stable isotopes and n-alkanes: modeling and application. Water Res. 197, 1–11.
Meng, L.Z., Hao, W.Y., Zhao, C., Li, J.H., Xue, J.Y., Li, J.H., Tu, L.Y., Huang, T., Yang, H., Yu, Z.Y., Yuang, L.W., Huang, C.C., 2023b. Anthropogenic activities generate high-refractory Black Carbon along the Yangtze River Continuum. Environ. Sci. Technol. 57 (23), 8598–8609.
Mesfioui, R., Abdulla, H.A.N., Hatcher, P.G., 2015. Photochemical alterations of natural and anthropogenic dissolved organic nitrogen in the York River. Environ. Sci. Technol. 49, 159–167.
Miller, B.L., Holtgrieve, G.W., Arias, M.E., Uy, S., Chheng, P., 2022. Coupled CH4 production and oxidation support CO2 supersaturation in a tropical flood pulse lake (Tonle Sap Lake, Cambodia). Proc. Natl. Acad. Sci. U.S.A. 119, 8.
Moosdorf, N., Renforth, P., Hartmann, J., 2014. Carbon dioxide efficiency of terrestrial enhanced weathering. Environ. Sci. Technol. 48, 4809–4816.
Qi, W.D., Müller, B., Pernet-Coudrier, B., Singer, H., Liu, H.J., Qu, J.H., Berg, M., 2014. Organic micropollutants in the Yangtze River: seasonal occurrence and annual loads. Sci. Total Environ 472, 789–799.
Qiao, W., Guo, H., He, C., Shi, Q., Zhao, B., 2021. Unraveling roles of dissolved organic matter in high arsenic groundwater based on molecular and optical signatures. J. Hazard. Mater. 406, 124–702.
Raymond, P.A., Hamilton, S.K., 2018. Anthropogenic influences on riverine fluxes of dissolved inorganic carbon to the oceans. Limnol. Oceanog. Letters 3, 143–155.
Raymond, P.A., Hartmann, J., Lauerwald, R., Sobek, S., McDonald, C., Hoover, M., Butman, D., Striegl, R., Mayorga, E., Humborg, C., Kortelainen, P., Dürr, H., Meybeck, M., Ciais, P., Guth, P., 2013. Global carbon dioxide emissions from inland waters. Nature 503, 355–359.
Raymond, P.A., Oh, N.H., Turner, R.E., Broussard, W., 2008. Anthropogenically enhanced fluxes of water and carbon from the Mississippi River. Nature 451, 449–452.
Ren, W., Tian, H., Tao, B., Yang, J., Pan, S., Cai, W.J., Lohrenz, S.E., He, R., Hopkinson, C.S., 2015. Large increase in dissolved inorganic carbon flux from the Mississippi River to Gulf of Mexico due to climatic and anthropogenic changes over the 21st century. J. Geophy. Res. 120, 724–736.
Richey, J.E., Melack, J.M., Aufdenkampe, A.K., Ballester, V.M., Hess, L.L., 2002. Outgassing from Amazonian rivers and wetlands as a large tropical source of atmospheric CO_2. Nature 416, 617–620.
Riedel, T., Zark, M., Vähätalo, A.V., Niggemann, J., Spencer, R.G.M., Hernes, P.J., Dittmar, T., 2016. Molecular signatures of biogeochemical transformations in dissolved organic matter from ten world rivers. Front Earth Sci 4, 85.
Rossel, P.E., Vahatalo, A.V., Witt, M., Dittmar, T., 2013. Molecular composition of dissolved organic matter from a wetland plant (Juncus effusus) after photochemical and microbial decomposition (1.25yr): common features with deep sea dissolved organic matter. Org. Geochem. 60, 62–71.
Shan, S., Luo, C., Qi, Y., Cai, W.J., Sun, S., Fan, D., Wang, X., 2021. Carbon isotopic and lithologic constraints on the sources and cycling of inorganic carbon in four large rivers in China: yangtze, Yellow, Pearl, and Heilongjiang. J. Geophy. Res. 126, e2020JG005901.
Shan, S., Qi, Y.Z., Luo, C.L., Fu, W.J., Xue, J.Y., Wang, X.C., 2020. Carbon isotopic constrains on the sources and controls of the terrestrial carbon transported in the four large rivers in China. Adv. Earth Sci 35 (9), 948–961. https://doi.org/10.11867/j.issn.1001-8166.2020.078.
Smith, D.F., Podgorski, D.C., Rodgers, R.P., Blakney, G.T., Hendrickson, C.L., 2018. 21 Tesla FT-ICR mass spectrometer for ultrhigh resolution analysis of complex organic mixtures. Anal. Chem. 90, 2041–2047.
Song, X.W., Lyu, S.D., Sun, K., Gao, Y., Wen, X., 2021. Flux and source of dissolved inorganic carbon in a headwater stream in a subtropical plantation catchment. J. Hydrol 600, 126511.
Spencer, R.G., Kellerman, A.M., Podgorski, D.C., Macedo, M.N., Jankowski, K., Nunes, D., Neill, C., 2019. Identifying the molecular signatures of agricultural expansion in Amazonian headwater streams. J. Geophys. Res. 124 (6), 1637–1650.
Spencer, R.G.M., Mann, P.J., Dittmar, T., Eglinton, T.I., McIntyre, C., Holmes, R.M., Zimov, Ni., Stubbins, A., 2015. Detecting the signature of permafrost thaw in Arctic rivers. Geophys. Res. Lett. 42 (8), 2015GL063498.
Stubbins, A., Lapierre, J.F., Berggren, M., Prairie, Y.T., Dittmar, T., Del Giorgio, P.A., 2014. What's in an EEM? Molecular signatures associated with dissolved organic Fluorescence in Boreal Canada. Environ. Sci. Technol. 48, 10598–10606.
Sun, X.N., Li, P.H., Zhou, Y.P., He, C., Cao, F., Wang, Y.T., Shi, Q., He, D., 2022. Linkages between optical and molecular signatures of dissolved organic matter along the Yangtze River Estuary-to- East China sea continuum. Front Mar. Sci 9, 933561.
Tank, S.E., Raymond, P.A., Striegl, R.G., McClelland, J.W., Holmes, R.M., Fiske, G.J., Peterson, B.J., 2018. A land-to-ocean perspective on the magnitude, source and implication of DIC flux from major Arctic rivers to the Arctic Ocean. Glob. Biogeochem. Cycles 26, 1–15.
Taylor, L.L., Quirk, J., Rachel, M.S., Thorley, P.A., Kharecha, J.H., Ridgwell, A., Lomas, M.R., Banwart, S.A., Beerling, D.J., 2016. Enhanced weathering strategies for stabilizing climate and averting ocean acidification. Nat. Clim. Chang 6, 402–406.
Telmer, K., Veizer, J., 1999. Carbon fluxes, pCO2 and substrate weathering in a large northern river basin, Canada: carbon isotope perspectives. Chem. Geol. 159, 61–86.
van Hoek, W.J., Wang, J.J., Vilmin, L., Beusen, A.H.W., Mogoll ó n, J.M., Pika, G.M., Philip, A., Liu, X.C., Langeveld, J.J., Bouwman, A.F., Middelburg, J.J., 2021. Exploring spatially explicit changes in Carbon budgets of global river basins during the 20th century. Environ. Sci. Technol. 55, 16757–16769.
Vaughn, D.R., Kellerman, A.M., Wickland, K.P., Striegl, R.G., Podgorski, D.C., Hawkings, J.R., Nienhuis, J.H., Dornblaser, M.M., Stets, E.G., Spencer, R.G.M., 2021. Anthropogenic landcover impacts fluvial dissolved organic matter composition in the Upper Mississippi River Basin. Biogeochemistry. https://doi.org/10.1007/s10533-021-00852-1.
Vorobev, A., Sharma, S., Yu, M.Y., Lee, J., Washington, B.J., Whitman, W.B., Ballantyne, F., Medeiros, P.M., Moran, M.A., 2018. Identifying labile DOM components in a coastal ocean through depleted bacterial transcripts and chemical signals. Environ. Microbiol. 20, 3012–3030.

Wagner, S., Riedel, T., Niggemann, J., Vähätalo, A.V., Dittmar, T., Jaffé, R., 2015. Linking the molecular signature of heteroatomic dissolved organic matter to watershed characteristics in world rivers. Environ. Sci. Technol. 49, 13798–13806.
Williams, C.J., Frost, P.C., Morales-Williams, A.M., Larson, J.H., Richardson, W.B., Chiandet, A.S., Xenopoulos, M.A., 2016. Human activities cause distinct dissolved organic matter composition across freshwater ecosystems. Glob. Chang. Biol 22, 613–626.
Williams, C.J., Yamashita, Y., Wilson, H.F., Jaffé, R., Xenopoulos, M.A., 2010. Unraveling the role of land use and microbial activity in shaping dissolved organic matter characteristics in stream ecosystems. Limnol. Oceanogr. 55, 1159–1171.
Wu, H., Li, J., Song, F., Zhang, Y., Zhang, H., Zhang, C., He, B., 2018. Spatial and temporal patterns of stable water isotopes along the Yangtze River during two drought years. Hydrolog. Proc.. 32, 4–16.
Yang, S.L., Milliman, J.D., Xu, K.H., Deng, B., Zhang, X.Y., Luo, X.X., 2014. Downstream sedimentary and geomorphic impacts of the Three Gorges Dam on the Yangtze River. Earth-Sci. Rev. 138, 469–486.
Ye, Q.H., Zhang, Z.T., Liu, Y.C., Wang, Y.H., Zhang, S., He, C., Shi, Q., Zeng, H.X., Wang, J.J., 2019. Spectroscopic and molecular-level characteristics of dissolved organic matter in a highly polluted urban river in South China. ACS Earth Space Chem 3, 2033–2044.
Zhang, J.T., Su, M.Z., Xi, B.D., Qian, G.R., Liu, J.Y., Hua, F., Huo, S.L., 2016a. Algal uptake of dissolved organic nitrogen in wastewater treatment plants. J. Environ. Manage. 50, 56–64.
Zhang, L., Peng, Y.Z., Ge, Z., Xu, K.C., 2019. Fate of dissolved organic nitrogen during the Anammox process using ultra-high resolution mass spectrometry. Environ. Int 131, 105042.
Zhang, L.J., Xue, M., Wang, M., Cai, W.J., Wang, L., Yu, Z.G., 2014. The spatiotemporal distribution of dissolved inorganic and organic carbon in the main stem of the Changjiang (Yangtze) River and the effect of the Three Gorges Reservoir. J. Geophy. Res. 119, 741–757.
Zhao, Z., Gonsior, M., Schmitt-Kopplin, P., Zhan, Y.C., Zhang, R., Jiao, N.Z., Chen, F., 2019. Microbial transformation of virus-induced dissolved organic matter from picocyanobacteria: coupling of bacterial diversity and DOM chemodiversity. ISME J. 13, 2551–2565.
Zheng, Q., Lin, W.X., Wang, Y., Li, Y.Y., He, C., Shen, Y., Guo, W.D., Shi, Q., Jiao, N.Z., 2020. Highly enriched N-containing organic molecules of Synechococcus lysates and their rapid transformation by heterotrophic bacteria. Limnol. Oceanogr 66, 335–348.
Zhou, C.X., Liu, Y.D., Liu, C.X., Liu, Y.Y., Tfaily, M.M., 2019. Compositional changes of dissolved organic carbon during its dynamic desorption from hyporheic zone sediments. Sci. Total Environ 658, 16–23.
Zhou, Y.Q., Yao, X.L., Zhou, L., Zhao, Z.H., Wang, X.L., Jang, K.S., Tian, W., Zhang, Y.L., Podgorski, D.C., Spencer, R.G.M., Kothawala, D.N., Jeppesen, E., Wu, F.C., 2021. How hydrology and anthropogenic activity influence the molecular composition and export of dissolved organic matter: observations along a large river continuum. Limnol. Oceanogr. 66, 1730–1742.
Zhou, Y.Q., Zhou, L., Zhang, Y.L., Zhu, G.W., Qin, B.Q., Jang, K., Spencer, R.G.M., Kothawala, D.N., Jeppesen, E., Brookes, J.D., Wu, F.C., 2022. Unraveling the role of anthropogenic and natural drivers in shaping the molecular composition and biolability of dissolved organic matter in non-pristine lakes. Environ. Sci. Technol. 56 (7), 4655–4664.